European Journal of Cancer 218 (2025) 115280

Contents lists available at ScienceDirect

European Journal of Cancer

journal homepage: www.ejcancer.com

Characterizing uveal melanoma patients with peritoneal metastases: A retrospective single-center analysis

Stanislav Rosnev [a], Caroline A. Peuker [a,b], Iris Piwonski [c], Jana Ihlow [b,c], Serge Leyvraz [a], Jonas Klingberg [a], David Horst [c], Maria Joosten [c], Markus Möbs [c], Antonia M. Joussen [d], Maximilian de Bucourt [e], Ulrich Keilholz [f,g], Ulrich Keller [a,g,h], Sebastian Ochsenreither [a,f,g], Susanne M. Rittig [a,b,*]

[a] Department of Hematology, Oncology and Cancer Immunology, Charité-Universitätsmedizin Berlin, Corporate Member of Freie Universität Berlin, Humboldt-Universität zu Berlin, and Berlin Institute of Health, Berlin, Germany
[b] Berlin Institute of Health at Charité-Universitätsmedizin Berlin, BIH Biomedical Innovation Academy, BIH Charité Clinician Scientist Program, Berlin, Germany
[c] Institute of Pathology, Charité-Universitätsmedizin Berlin, Corporate Member of Freie Universität Berlin, Humboldt-Universität zu Berlin, and Berlin Institute of Health, Berlin, Germany
[d] Department of Ophthalmology, Charité-Universitätsmedizin Berlin, Corporate Member of Freie Universität Berlin, Humboldt-Universität zu Berlin, and Berlin Institute of Health, Berlin, Germany
[e] Department of Diagnostic and Interventional Radiology, Charité-Universitätsmedizin Berlin, Corporate Member of Freie Universität Berlin, Humboldt-Universität zu Berlin, and Berlin Institute of Health, Berlin, Germany
[f] Charité Comprehensive Cancer Center, Charité-Universitätsmedizin Berlin, Corporate Member of Freie Universität Berlin, Humboldt-Universität zu Berlin, and Berlin Institute of Health, Berlin, Germany
[g] German Cancer Consortium (DKTK) partner site Berlin and German Cancer Research Center (DKFZ), Heidelberg, Germany
[h] Max-Delbrück-Center for Molecular Medicine, Berlin, Germany

ARTICLE INFO

Keywords:
Uveal melanoma
Peritoneal metastases
Monosomy
BAP1
Checkpoint inhibitors
Survival
Prognosis

ABSTRACT

Background: Metastatic uveal melanoma (mUM) is an aggressive cancer predominately affecting the liver. Peritoneal metastases (PM) occur rarely, and there is limited knowledge about this subgroup's clinical course and biology.

Methods: We analyzed 41 mUM patients with confirmed PM from the Charité-Universitätsmedizin Berlin database, focusing on clinical characteristics, immune cell infiltrates, genetic alterations and tumor mutational burden (TMB).

Results: The incidence of PM in mUM was 4.27 %. Metastatic disease was diagnosed 3.6 years after primary UM, with PM developing later (median: 4.7 years). Median overall survival (OS) from mUM diagnosis was 22.4 months. Prognosis correlated with metastatic pattern. Patients presenting with synchronous liver and peritoneal metastases or primary hepatic metastases followed by secondary peritoneal dissemination showed a median OS of 19.7 and 17.7 months, respectively. However, PM patients with exclusive extrahepatic disease at diagnosis of mUM had a significantly longer OS of 48.6 months and this metastatic pattern showed highly significant correlation with low and intermediate genetic risk. Metastasis-free survival and OS upon mUM diagnosis were significantly shorter in patients with high-risk UM tumors. TMB also correlated with metastatic pattern, being lowest in patients presenting with only extrahepatic disease. Higher TMB was generally associated with shorter OS.

Conclusion: PM in mUM patients is rare and in contrast to other extra-abdominal tumors does not worsen prognosis. Prognosis is greatly influenced by the metastatic pattern, which is determined by tumor biology, as evidenced by its correlation with genetic risk groups and TMB.

* Correspondence to: Department of Hematology, Oncology and Cancer Immunology, Campus Benjamin Franklin, Charité-Universitätsmedizin Berlin, Hindenburgdamm 30, Berlin 12203, Germany
E-mail address: susanne-malaika.rittig@charite.de (S.M. Rittig).

https://doi.org/10.1016/j.ejca.2025.115280
Received 2 September 2024; Received in revised form 29 January 2025; Accepted 31 January 2025
Available online 6 February 2025

1. Introduction

In patients with primary uveal melanoma (pUM) metastases occur in approximately 50 % of all patients [1], typically within a median time of three years after local treatment of the primary tumor in the eye [2,3]. However, tumor spread can arise after a decade or longer [4]. The most common sites of metastases in UM include liver (93 %), lung (24 %), bone (16 %), skin/subcutaneous tissue (11 %), lymph nodes (8–38 %), and the brain (5–6 %) [5,6]. Metastatic uveal melanoma (mUM) is associated with poor prognosis. Median survival ranges from 12 to 17 months [7,8], however, it can be significantly longer in certain subgroups of patients [9], and currently, only limited treatment options are available.

Biallelic inactivation of the gene encoding BRCA1-associated protein 1 (BAP1) on chromosome 3p21.1 occurs in approximately 50 % of pUM, mainly through loss of heterozygosity 3. An additional deleterious somatic mutation of the second BAP1 allele is associated with a higher risk of metastatic disease and poor prognosis in the metastatic setting [10,11]. The UM tumor microenvironment has the least immune cell infiltration of all cancer types studied in The Cancer Genome Atlas [12]. UM is further characterized by one of the lowest mutational burdens in solid cancer [13,14]. Only a minority of tumors, especially those with monosomy 3 and biallelic BAP1 loss, show considerable immune infiltration [15] which, however, is not associated with a better prognosis [15,16]. The immune-privileged intraocular microenvironment of the primary tumor and, in metastatic disease, the intrahepatic immunological tolerance may play an important role regarding the observed inefficient antitumor immune responses [15-18].

Systemic treatment of mUM is characterized by extremely poor response rates to conventional chemotherapy. In contrast to cutaneous melanoma (CM), targeting molecular alterations, i.e. activated downstream effectors of Gαq/11 such as the mitogen-activated protein kinase (MAPK) pathway, has shown only limited benefit with available inhibitors [7]. Moreover, immune checkpoint inhibitors approved for the treatment of CM are considerably less effective in mUM [19,20]. Given the limited activity of systemic therapies and the strong hepatotropism of mUM, liver-directed therapies such as transarterial chemoembolization (TACE) or selective internal radiotherapy (SIRT) are applied with moderate success [21]. Tebentafusp, a gp100-targeting T cell redirecting bispecific fusion protein, is the first agent conferring an overall survival (OS) benefit in treatment-naïve and pretreated mUM patients [8,22]. Yet, treatment with tebentafusp is limited to HLA-A* 02:01-positive patients [23]. Due to restricted therapeutic options and the heterogeneous courses of disease, individual treatment strategies are usually pursued.

PM occurs quite frequently in ovarian, gastric, and colorectal cancer, and is associated with dismal prognosis [24,25]. On the contrary, extra-abdominal tumors only rarely spread to the peritoneum, but PM is seen especially in breast, lung, kidney cancer, and CM [26,27]. Only little data is available on prognosis in these cases, but OS upon diagnosis of PM ranges from one to six months with the longest documented survival in breast cancer. However, in breast cancer, occurrence of PM tremendously impairs prognosis. In intraperitoneal tumors, PM is thought to develop by detachment of tumor cells, then breaking through the serosa. Tumor cells may also be spread during surgery and can further scatter from existing peritoneal implants via the peritoneal fluid. Cells originating from extra-abdominal tumors can enter the peritoneum after breaking into lymph and/or blood vessels. However, the pathophysiology of PM in these tumors is not well understood. Several aspects contribute to the development of PM including the high vascularization of the peritoneum. The expression of adhesion molecules in mesothelial cells of secondary lymphoid organs located in the omentum (termed "milky spots") allows cancer cells to attach. Further, a pre-metastatic niche is created when so-called neutrophil-extracellular traps (NETs) develop. NETs contain DNA derived from neutrophils which can enhance motility of cancer cells by interaction with their cell membrane. Moreover, the expression of inhibitory immune checkpoints on macrophages and cytotoxic T cells contributes to an immunosuppressive environment [24].

So far, no reliable data has been published on the tumor biology or course of disease in patients with peritoneally disseminated mUM. In this retrospective study, we summarized clinical data available at our center regarding this patient subpopulation, described metastatic patterns, correlated genetic risk groups and tumor mutational burden (TMB) where possible, and further described the immune cell infiltration of the tumor microenvironment in available tumor samples.

2. Methods

2.1. Patients

Information was gained from patients treated between 2004 and 2022 and archived in the medical database of Charité-Universitätsmedizin Berlin. Screening of the database was performed following institutional review board approval (EA4/034/21). Patients with peritoneal metastases (PM) of UM, diagnosed according to radiological (CT scan, N = 23 (56.1 %); MRI scan, N = 14 (34.1 %)) and/or histopathological findings (N = 4 (9.8 %)), were identified and included in the analysis. At the time of data analysis in February 2024 90.2 % (N = 37) of patients were deceased. In 14 patients (34.1 %), initial diagnosis of mUM was established during regular surveillance after local treatment of pUM. In eight patients (19.5 %) diagnostic evaluations for mUM was prompted by newly occurring symptoms, while for the remaining patients (N = 19, 46.3 %), information regarding the initial diagnosis setting – whether it was through systemic surveillance, clinical symptoms, or incidental findings – was not available. During subsequent treatment, systemic follow-up included CT of the chest and abdominal MRI every two to three months, as well as additional imaging where tumor progression was clinically suspected. In cases of only hepatic dissemination abdominal MRI scans were performed every two to three months and CT scans including the chest were performed every five to six months.

2.2. Study design

Data regarding patient demographics, tumor characteristics, disease and treatment history, and patient outcomes were obtained. Regular radiological imaging was conducted in all patients undergoing systemic and liver-directed treatment as described above. Peritoneal sampling and/or paracentesis were performed in some cases to verify peritoneal affection. Primary endpoint was the assessment of median OS of mUM patients with PM. Secondary objectives included determining the median OS from diagnosis of pUM and PM, response to immune checkpoint blockade (ICB), clinical characteristics, pattern of metastases, as well as analyses of the relationship between the metastatic pattern and genetic risk groups and TMB. We further descriptively analyzed the immune cell infiltration of the tumor microenvironment in available hepatic and peritoneal tumor samples.

2.3. Immunohistochemistry

4μm sections of paraffin-embedded (FFPE) UM metastases were stained with hematoxylin-eosin (H&E) and immunohistochemically analyzed using an automated Ventana BenchMark XT immunostainer (Ventana Medical Systems, Inc., Tucson, AZ, USA) and a Leica Bond MAX system (Leica Biosystems, Buffalo, NY, USA). Tissue sections were deparaffinized, rehydrated, and subjected to heat-induced epitope retrieval and endogenous peroxidase blocking using H_2O_2. FFPE slides were incubated with antibodies for BAP1, ki67, PD-L1, CD3, CD4, CD68, PAX5, CD56, FOXP3, MPO, CD123, CD11c, as outlined in Table S1. This was followed by chromogen 3,3′-diaminobenzidine tetrahydrochloride (UV-DAB) application and counterstaining with hematoxylin. Whole

slides were examined by two pathologists independently. For evaluation of the immune microenvironment, immune cell types were assessed regarding their surface antigen expression, distribution pattern, and localization. Cell quantities were assessed as percentage of all cells within the tumor area and the direct tumor surrounding. The $CD4^+$ and $CD8^+$ T cell ratios were presented as percentage of all $CD3^+$ T cells. The ratio of $CD11c^+$ macrophage was estimated as percentage of all macrophages. Tumor cells with nuclear BAP1 expression (any staining intensity) were considered BAP1 positive. PD-L1 tumor cell (TC) score was measured as percentage of positive tumor cells, PD-L1 immune cell (IC) score was measured as percentage of immune cells within the entire tumor area. Combined Positive Score (CPS) was calculated as follows: positive tumor cells and immune cells / tumor area x 100.

2.4. Molecular analysis

Tissue sections were deparaffinized with xylene and ethanol and the tumor areas were macrodissected with a scalpel. DNA was extracted semi-automatically using the Maxwell RSC DNA FFPE kit on a Maxwell® RSC 48 according to manufacturer's instructions (Promega, Madison, WI, USA). All DNA samples were analyzed using hybrid capture-based next-generation sequencing technology (Agilent XT HS2) using the SureSelect Cancer Comprehensive Genomic Profiling Assay (CGP Assay, Agilent Technologie, Santa Clara, CA, USA). Library preparation was performed fully automated on a Magnis NGS Prep System (Agilent Technologies). Sequencing was performed on a NextSeq 2000 (Ilumina Inc., San Diego, CA, USA). For the mutation analysis, the data from the focused DNA NGS were evaluated with the DRAGEN-Bio-IT platform (Ilumina) and variants with an allele frequency of ≥ 3 % were considered. Allele-specific copy number variation (CNV) analysis was performed using pureCN as described in Willing et al. [28]. The calculation of the tumor mutation burden is based on Chalmers et al. [29] including all synonymous and non-synonymous, presumably somatic variants with an allele frequency of > 3 %. To exclude potential germline variants, all variants were compared with entries in the "Database of Single Nucleotide Polymorphisms (dbSNP)" and the "Genome Aggregation Database (gnomAD)" and filtered out if necessary. In addition, known driver mutations with > 100 entries in "COSMIC, The Catalog Of Somatic Mutations In Cancer" were not included in the calculation.

2.5. Statistical analysis

Due to low patient numbers, both continuous and categorical variables were summarized with non-parametric descriptive statistics. Cox regression analysis was performed to assess OS and PFS in all patients and for specific patient subgroups. P-values of < 0.05 were considered statistically significant. Statistical analysis was performed using GraphPad Prism version 10.2.3s. Respective methods are indicated in the figure legends. Analyses were considered exploratory, and therefore no adjustment for multiple testing was performed.

3. Results

3.1. Patient characteristics

Between 2004 and 2022 a total of 960 mUM patients were treated at our center. Among these patients, we identified N = 41 patients with PM, which results in a PM frequency of 4.27 %. The median age at pUM and mUM diagnosis was 58 years (range: 35–77) and 64 years (range: 44–80), respectively. In median, three treatment lines were administered in metastatic disease. The most frequently used liver-specific treatment modalities were TACE and SIRT. 41.5 % (N = 17) of patients received ICB treatment at some point during the course of metastatic disease (Table 1).

Table 1
Overview of patient characteristics. DTIC, dacarbazine; IHP, isolated hepatic perfusion; mUM, metastatic uveal melanoma; PM, peritoneal metastases; pUM, primary uveal melanoma; PD1, programmed cell death protein 1; RFA, radiofrequency ablation; SIRT, selective intrahepatic radiotherapy; TACE, transarterial chemoembolization.

	Number of Patients	%
Sex		
Male	29	70.7
Female	12	29.3
Number of systemic treatments for mUM		
0	4	9.7
1	16	39
2	10	24.5
3	6	14.6
≥ 4	5	12.2
Liver-specific treatments		
TACE	19	46.3
SIRT	14	34.1
Other (RFA, IHP, surgery)	3	7.3
Systemic treatments		
Gemcitabin/treosulfan	24	58.5
Ipilimumab/nivolumab	12	29.2
Fotemustin	9	21.9
Tebentafusp	8	19.5
Trametinib	5	12.2
Anti-PD1	5	12.2
Other (sorafenib, crizotinib, DTIC)	6	14.6
Median age	**(years)**	**(range)**
At pUM diagnosis	58	35–77
At mUM diagnosis	64	44–80
Patient cohorts		
(A) Initial extrahepatic spread	6	14.6
(B) Synchronous hepatic/peritoneal spread	9	22.0
(C) Primary hepatic and sequential peritoneal spread	26	63.4

3.2. Course of disease and metastatic pattern

The median time from primary to metastatic UM diagnosis was 3.6 years, while the median time to development of PM from primary diagnosis was 4.7 years and 12.8 months from mUM (range: 1.5–123.3; N = 26) (Figs. 1A/B and S1). The median number of affected organ systems at the time of initial diagnosis of metastatic disease was two (Fig. 2A) compared to four at PM detection (Fig. 2B). 29.3 % (N = 12) of patients presented with primary peritoneal dissemination. No sole PM as the initial manifestation of mUM was observed in any patient. We also did not see any striking differences in patterns of metastases in patients with primary PM compared to patients with secondary PM (Table S2). Table S2 contains detailed information on the specific metastatic sites in each patient.

3.3. General and cohort-specific overall survival

The median OS upon diagnosis of mUM for all patients was 22.4 months (95 % CI: 13.2–31.6; Fig. 3A) and 7.7 months upon diagnosis of PM (95 % CI: 3.8–11.6; Fig. 3B). Further, OS was analyzed in three different patient cohorts according to the temporal occurrence of metastatic sites: Cohort A comprised patients where PM was diagnosed in the absence of liver metastases (14.6 %, N = 6). In cohort B, patients developed synchronous liver and peritoneal metastases (22 %, N = 9), while in cohort C patients presented with primary hepatic metastases followed by secondary peritoneal dissemination (63.4 %, N = 26). Definition of the three cohorts is stated in Table 1

Patients in cohort A showed a 1-year survival rate of 100 % after diagnosis of mUM with a median OS of 48.6 months (95 % CI: 2.2–95.0; Fig. 3C), which was significantly longer compared to patients with initial hepatic metastases regardless of temporal occurrence of PM (cohort B + cohort C; N = 35 (85.4 %); p = 0.0196). The 1-year survival

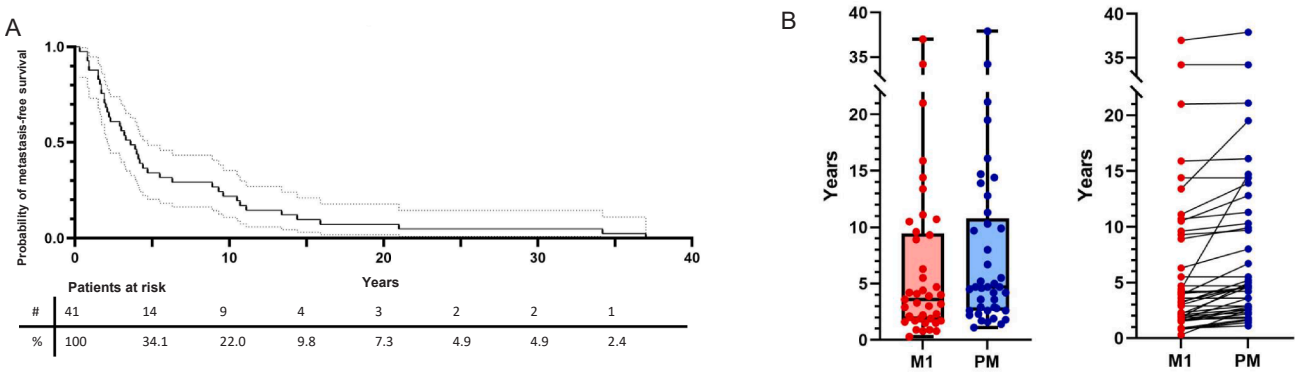

Fig. 1. Time from primary to metastatic UM and peritoneal metastases. (A) Kaplan-Meier plot representing metastasis-free survival from primary UM diagnosis (median: 3.6 years; range: 0.8–37 years; N = 41), (B) Boxplots representing time from primary diagnosis to detection of metastatic disease at any location (M1, red: median: 3.6 years; range: 0.8–37 years; N = 41) and time from primary diagnosis to development of peritoneal metastases (PM, blue: median: 4.7 years; range: 1.1–37.8; N = 41). Right: Boxplots representing individual data regarding temporal occurance of metastatic disease at any location (red) and development of peritoneal metastases (blue).

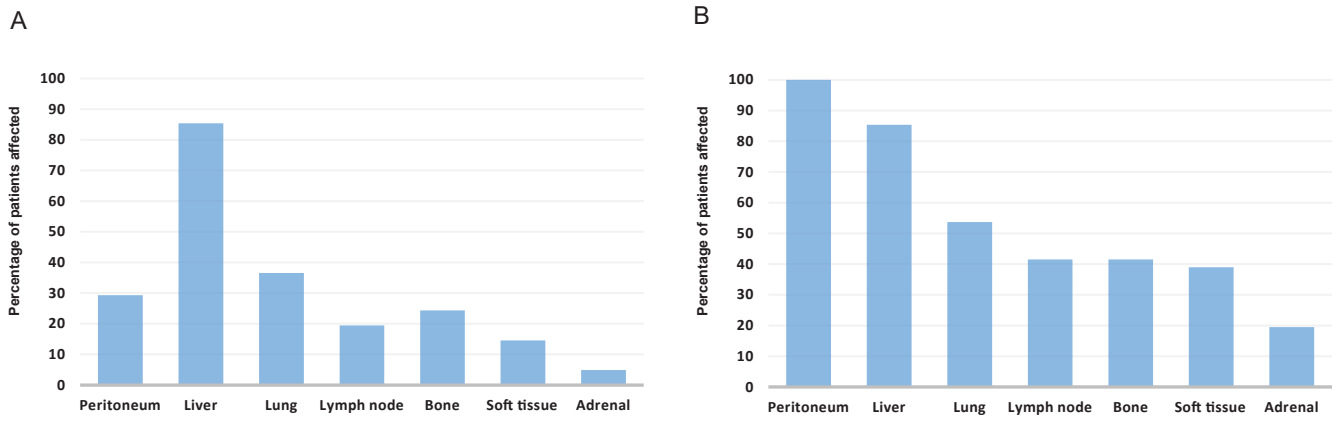

Fig. 2. Overview of metastatic dissemination in the course of disease. (A) affected organ systems at initial diagnosis of metastatic disease (median: 2; range: 1–7): peritoneum (29.3 %, N = 12), liver (85.4 %; N = 35), lungs (36.6 %; N = 15), lymph nodes (19.5 %; N = 8), bone (24.4 %; N = 10), soft tissue (14.6 %; N = 6), adrenal glands (4.9 %; N = 2); (B) affected organ systems at diagnosis of peritoneal metastases (median: 4; range: 2–8): peritoneum (100 %, N = 41), liver (85.4 %; N = 35), lungs (53.7 %; N = 22), lymph nodes (41.5 %; N = 17), bone (41.5 %; N = 17), soft tissue (39.0 %; N = 16), adrenal glands (19.5 %; N = 8).

rate in cohort B was 80.6 % compared to 55.5 % in cohort C. However, the distinction of temporal occurrence of PM was not associated with a significant difference in OS (19.7 months cohort B vs. 17.7 months cohort C, p = 0.6178; Fig. S2).

To evaluate possible correlations between the metastatic pattern and course of disease, the time from primary diagnosis to mUM diagnosis and PM detection was analyzed in these three patient subgroups (Fig. S3A/B). Although differences were not statistically significant, the time from the primary diagnosis to the development of metastatic disease was longer in cohort A (PM in the absence of hepatic metastases) with an average of 7.5 years, compared to 4.2 years in cohort B, and 2.25 years in cohort C.

3.4. Analysis of immune cell composition

In order to identify potential differences in immune cell infiltration between the two metastatic sites peritoneum and liver, we performed immune profiling by immunohistochemistry. In 10 mUM patients, sufficient tumor material with adequate quality was available. Nine were derived from hepatic metastases and one was derived from a peritoneal metastasis. An overview of the immune cell composition in the studied samples is given in Table 2. T-cell infiltration of varying extents was observed in all samples derived from hepatic lesions. The ratio between $CD4^+$, and $CD8^+$ T cells was skewed ($CD4^+/CD8^+$ ratio 0.05–4.0) with a tendency towards equal or near equal ratio (N = 4) or $CD8^+$ T cell excess (N = 4). Similarly, in all liver samples macrophages could be detected, and were mostly diffusely distributed intratumorally as well as in the surrounding healthy tissue. In the majority of liver samples, macrophages were predominantly $CD11^+$. In six out of nine hepatic samples, low rates of B-cell infiltrates could be detected, whereas NK cells were identified in only 2/9 and Tregs in 3/9 samples. Only one sample showed a positive IC score of 1 %. The examined peritoneal mUM sample showed similar immune profile characteristics with a low T-cell infiltration and diffusely distributed T cells intratumorally, as well as at the tumor's edge. $CD8^+$ T cells comprised the majority of all $CD3^+$ cells in this sample. Macrophages were diffusely distributed in the tumor and the surrounding tissue. The quantity and percentage of $CD11^+$ macrophages were lower compared to the liver samples. We further did not see any relevant differences regarding the immune infiltration in UM liver metastases depending on their syn-/metachronous timing of occurrence (Table 2). Fig. 4 shows representative stainings of three patients with simultaneous hepatic and peritoneal mUM dissemination.

3.5. Molecular characteristics and association with prognosis

In 22 patients we conducted next-generation sequencing (NGS) analysis in available FFPE tumor samples to assess genetic risk groups regarding prognosis. Table 3 displays a summary of the relevant genetic

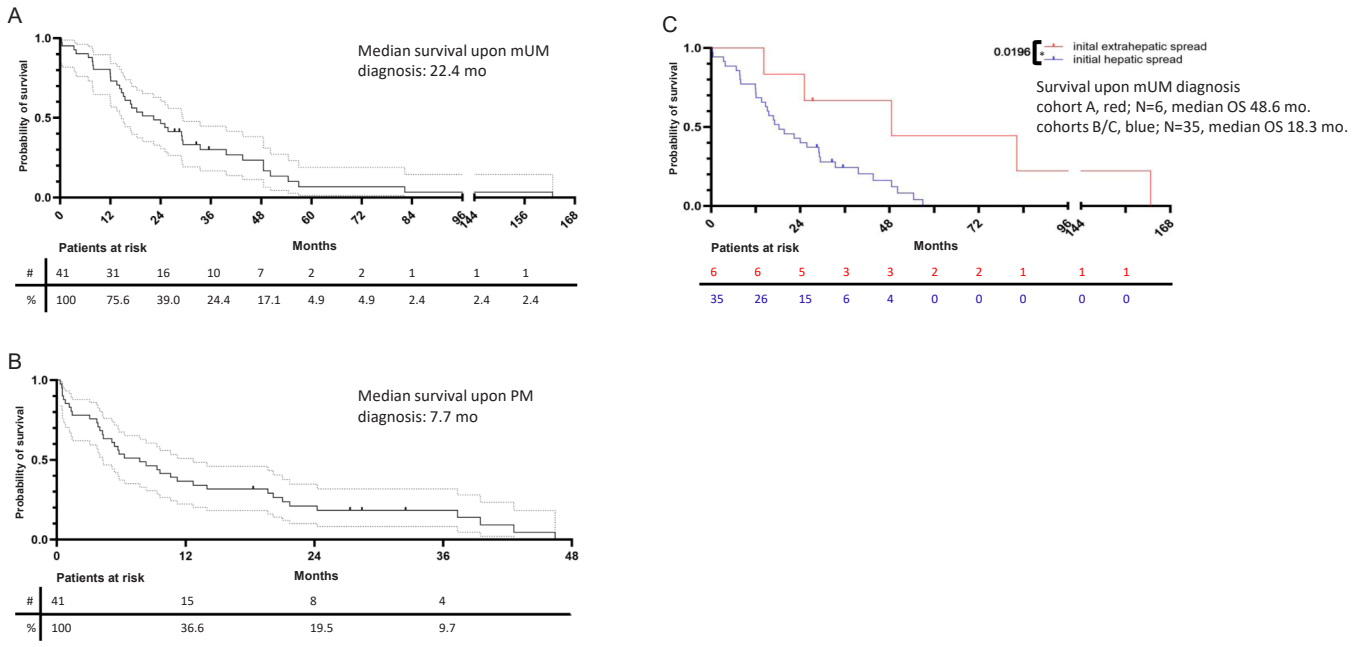

Fig. 3. Overall survival. Kaplan-Meier survival plots representing (A) the median overall survival of all patients upon initial diagnosis of metastatic uveal melanoma (median 22.4 months; 95 % CI: 13.2–31.6; N = 41); (B) the median overall survival of all patients upon initial diagnosis of peritoneal metastases (median 7.7 months; 95 % CI: 3.8–11.6; N = 41); (C) the median overall survival of patients with initial extrahepatic dissemination (cohort A, red; median 48.6 months; 95 % CI: 2.2–95.0; N = 6) vs. patients with initial hepatic metastases (cohorts B and C, blue; 18.3 months; 95 % CI: 12.9–23.7; N = 35). Log-rank (Mantel Cox) test: p = 0.0196; Initial extrahepatic sites in cohort A included the following at the timepoint of mUM diagnosis: PER, OSS, PUL, PLE, LYM, OTH (pancreas). Detailed information on metastatic sites is depicted in Table S2.

alterations, risk group classification according to Jager et al. [1], and tumor material characteristics. Table S3 contains more detailed information on genetic findings.

Regarding the well-defined tumor genetic risk classification for prognosis in UM into low, intermediate, and high-risk groups based on CNVs of chromosomes 3, 8 and 6, as well as somatic mutations in key genes of interests such as BAP1/SF3B1/EIF1AX [1], an analysis of 22 tumor samples revealed the following distribution in our patients: three (13.6 %) were classified as low genetic risk, three (13.6 %) as intermediate, and 17 (72.8 %) as high risk.

Notably, cohort A had a significantly higher frequency of low and intermediate risk tumors compared to cohorts B and C (p = 0.0038, Fig. 5A). To investigate the relationship between the genetic characteristics of UM and the clinical course of disease, we compared patients with low/intermediate genetic risk (N = 6) to those with high genetic risk (N = 16) in regard to time to mUM and PM diagnosis. The median time from pUM to mUM and pUM to PM diagnosis in the low/intermediate genetic risk group was notably longer with 11.95 and 14.55 years compared to 2.05 and 2.7 years in the high-risk group, respectively (p = 0.0277 and p = 0.0183; Fig. 5B/C).

Additionally, when comparing OS upon mUM diagnosis, we observed a highly significant difference favoring the low/intermediate risk group, with a median OS of 40.5 months compared to 15.3 months in the high-risk patient group (p = 0.009, Fig. 5D).

The median TMB in the entire patient group was 1.72 mut/Mb (range: 7.46). Interestingly, we observed a statistically significant correlation between higher TMB and shorter OS from mUM diagnosis (p = 0.041, Fig. S4A). However, there was no correlation between TMB and the time between pUM and the onset of metastatic disease or occurrence of PM, respectively (data not shown). A comparison between the three patient cohorts (A/B/C) regarding TMB revealed significantly lower TMB in patient cohort A with initial sole extrahepatic metastases compared to patient cohort C where liver metastases presented first (p = 0.021, Fig. S4B).

3.6. Response to immune checkpoint blockade

The cohort-specific treatment response in patients undergoing ICB treatment was analyzed. Four out of six patients with initial extrahepatic spread only (cohort A) received ICB in the course of mUM (N = 2 ipilimumab/nivolumab, N = 2 anti-PD1 monotherapy) in comparison to 13 out of 35 patients of cohorts B and C (N = 10 ipilimumab/nivolumab, N = 3 anti-PD1 monotherapy, one patient was excluded from the analysis as the treatment was discontinued after the first ICB application due to immune-related toxicity). Median PFS in cohort A was 6.5 months compared to 3.5 months in cohorts B and C while the difference was not statistically significant (p = 0.1677; Fig. S5). No correlation could be seen between PFS under ICB treatment and TMB, however, TMB data were only available in 10 of the ICB-treated patients (data not shown). We further did not observe any correlation between the number of treatment lines in general and median OS in our patient cohort.

4. Discussion

PM in mUM is a rare occurrence in the context of an overall rare tumor entity. To our knowledge, this is the first analysis of the clinical course and characteristics of this patient subgroup and we for the first time present an estimated incidence of 4 % for PM in mUM. In general, the development of PM in extra-abdominal cancers is known to occur in advanced stages of metastatic disease and is associated with adverse prognosis [24,26,27,30,31]. Similarly to PM in other extra-abdominal cancers, in our cohort, PM tended to occur late during the course of metastatic disease, which was also reflected by multi-organ metastatic involvement at the time of PM diagnosis. However, in strong contrast to other cancer entities including CM, this did not affect prognosis. With 22.4 months, the median OS in our cohort was markedly longer than the reported median OS of 10–19 months of UM patients with metastatic disease in general [32,33,7]. The median OS of patients treated with first-line tebentafusp represents the patient cohort with the longest reported OS in mUM in a prospective phase III trial (21.7 months vs. 16.0

Table 2
Tumor immune cell composition. Immune cell type-specific quantities (quant.) were determined as percentage of all cells within the tumor area and the direct tumor surrounding. CD4/CD8-ratio was determined as percentage of all $CD3^+$ T cells. For PD-L1 assessment, at least 100 vital tumor cells were considered sufficient and any membranous staining of either tumor- or immune cells was considered positive, regardless of the intensity and completeness of the staining result. All samples had a PD-L1 TC (Tumor Cells) score of 0.

Patient/ Cohort	Location	ki67	T cell quant.	T cell distribution	CD4 (% of all T cells)	CD8 (% of all T cells)	Macrophage quant.	Macrophage distribution	$CD11c^+$ macrophages (of all macrophages)	B cell quant.	NK cell quant.	Treg quant.	Granulocyte quant.	Quant. of plasmacytoid dendritic cells	PD-L1
B2	hepatic	5 %	1–5 %	diffusely interstitial and intratumoral	5 %	95 %	6–10 %	small aggregates at tumor edge, diffusely intratumoral	30 %	1–5 %	0 %	1–5 %	1–5 %	1–5 %	CPS 0
B6	hepatic	1 %	6–10 %	small aggregates at tumor edge	50 %	50 %	6–10 %	diffusely distributed intratumoral and in healthy tissue	50 %	1–5 %	0 %	0 %	1–5 %	0 %	CPS 0
C1	hepatic	2 %	6–10 %	small aggregates at tumor edge, few diffusely intratumoral	50 %	50 %	6–10 %	diffusely distributed intratumoral and in healthy tissue	100 %	1–5 %	0 %	0 %	1–5 %	1–5 %	CPS 0
C3	hepatic	< 1 %	6–10 %	aggregate and diffuse distribution	5 %	95 %	1–5 %	diffusely distributed at tumor edge, intratumoral and in healthy tissue	0 %	0 %	0 %	0 %	1–5 %	0 %	CPS 0
C4	hepatic	2 %	6–10 %	small aggregate at tumor edge, few diffusely intratumoral	80 %	20 %	6–10 %	diffusely distributed intratumoral and in healthy tissue	70 %	0 %	0 %	0 %	0 %	0 %	CPS 0
C8	hepatic	1 %	6–10 %	aggregate at tumor egde	50 %	50 %	6–10 %	aggregates at tumor edge, diffusely distributed in healthy tissue	100 %	1–5 %	1–5 %	1–5 %	1–5 %	0 %	CPS 0
C12	hepatic	< 1 %	6–10 %	diffusely distributed intratumoral and at tumor edge	20 %	80 %	6–10 %	diffusely distributed intratumoral	90 %	1–5 %	1–5 %	1–5 %	1–5 %	1–5 %	CPS 0
C17	hepatic	< 1 %	1–5 %	diffusely distributed	none	100 %	1–5 %	diffusely distributed intratumoral and in healthy tissue	100 %	0 %	0 %	0 %	0 %	0 %	CPS 0
C21	hepatic	< 1 %	6–10 %	diffusely distributed intratumoral; aggregates at tumor edge	40 %	60 %	6–10 %	diffusely distributed intratumoral, aggregates in healthy tissue	100 % + dendritic cells in aggregates	1–5 %	0 %	0 %	1–5 %	0 %	CPS 1
B5	peritoneal	< 1 %	1–5 %	diffusely distributed intratumoral and at tumor edge	20 %	80 %	1–5 %	diffusely distributed intratumoral and in healthy tissue	5 %	1–5 %	0 %	0 %	1–5 %	0 %	CPS 0

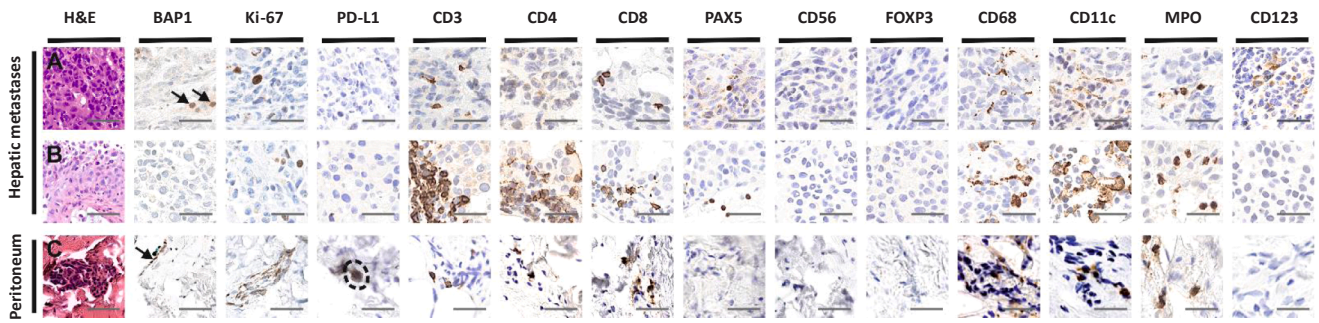

Fig. 4. Histopathology and immunohistochemistry of peritoneal and hepatic uveal melanoma metastases. Liver (panel A and B, scale bar 85 μm) and peritoneum (panel C, scale bar 175 μm). H&E stain shows epitheloid melanoma infiltrates with intracytoplasmic and intertumoral deposition of melanin pigment. Nuclear BAP1 expression is absent in all three tumor samples while healthy liver parenchyma and mesothelial cells show positive nuclear staining results (arrows). The proliferation index as measured by nuclear ki-67 expression is $\leq$ 5 % in all three samples. PD-L1 is consistently negative, in both tumor cells and immune cells. Melanin pigment (encircled) should not be confused with positive PD-L1 staining results. In comparison with sample A and C, sample B is enriched in T cells as highlighted by membranous CD3-stain and CD4:CD8-relation is highest in this patient. In comparison with the peritoneal metastasis, only a few B cells are present within the two liver metastases as highlighted by nuclear PAX5-stain. In all three samples, Tregs (FOXP3) and NK cells (CD56) are completely absent. Moreover, macrophage infiltration is higher in the two liver metastases as highlighted by CD68- and CD11c stains. The second liver metastasis shows a particularly high amount of $CD11c^+$ activated macrophages. Since $CD11c^+$ cells outnumber $CD68^+$ cells, the presence of $CD11c^+$ dendritic cells amongst the tumor microenvironment is likely in this sample. All three metastases show few intermixed granulocytes as highlighted by the MPO stain. CD123 stain reveals few plasmacytoid dendritic cells in sample A.

Table 3
Molecular characteristics and risk group classification. Summary of relevant genetic characteristics (CNVs and somatic mutations) of 22 patients, risk group classification based on identified genetic alterations, tumor mutational burden (TMB) and details regarding origin of sampled tissue. D3, disomy 3. LOH, loss of heterozygosity. M3, monosomy 3. WT, wild type.

Patient/ Cohort	Risk group	Site of sampling	Chr 3 based on Chr 3p and 3q	Chr 8q	Chr 6p	EIF1AX	SF3B1	SRSF2	TMB
A1	high	OSS	M3	three or more copies gain	total gain	WT	WT	WT	0,57
A2	low	OTH (soft tissue)	D3	mixed (partial gains and losses)	partial gain(s)	WT	WT	WT	1,72
A4	intermediate	LYM	D3	partial three or more copies gain	total gain	WT	WT	WT	1,72
A5	low	PER	D3	no abnormalities	partial gain(s)	exon 1: c.5C>T; p.P2L	WT	WT	1,15
A6	intermediate	OSS	mixed	partial three or more copies gain	total gain	WT	exon 5: c.1873C>T; p.R625C	WT	0,57
B2	high	HEP	M3	total gain	partial gain(s)	WT	WT	WT	8,03
B4	high	PER	M3	total gain	total gain	WT	exon 5: c.1873C>T; p.R625C	WT	2,87
B6	high	HEP	M3	three or more copies gain	partial gain(s)	WT	WT	WT	4,01
B7	intermediate	OTH (soft tissue)	D3	total gain	total gain	exon 1: c.5C>T; p.P2L	exon 14: c.1997A>C; p.K666T	WT	1,72
B8	high	primary	M3	total gain	partial gain(s)	WT	WT	WT	0,57
B9	high	OSS	M3	three or more copies gain	partial gain(s)	WT	WT	WT	1,72
C1	high	HEP	M3	no abnormalities	partial gain(s)	exon 2: c.17G>A; p.G6D	WT	WT	2,87
C2	high	HEP	allelic imballance LOH	three or more copies gain	total gain	WT	WT	WT	1,72
C4	high	HEP	M3	three or more copies gain	partial gain(s)	WT	WT	WT	1,72
C6	high	primary	M3	total gain	partial gain(s)	WT	WT	WT	4,59
C8	high	HEP	M3	partial three or more copies gain	partial gain(s)	WT	WT	WT	1,72
C11	high	OTH (soft tissue)	LOH	partial three or more copies gain	total gain	WT	WT	WT	0,57
C18	low	HEP	D3	total gain	total gain	exon 4: c.208T>C; p.W70R	WT	WT	2,87
C19	high	LYM	M3	total gain	partial gain(s)	WT	WT	WT	2,29
C21	high	HEP	M3	three or more copies gain	partial gain(s)	WT	WT	WT	5,16
C22	high	HEP	LOH	total gain	total gain	WT	WT	WT	4,01
C23	high	HEP	M3	total gain	no abnormalities	WT	WT	WT	3,44

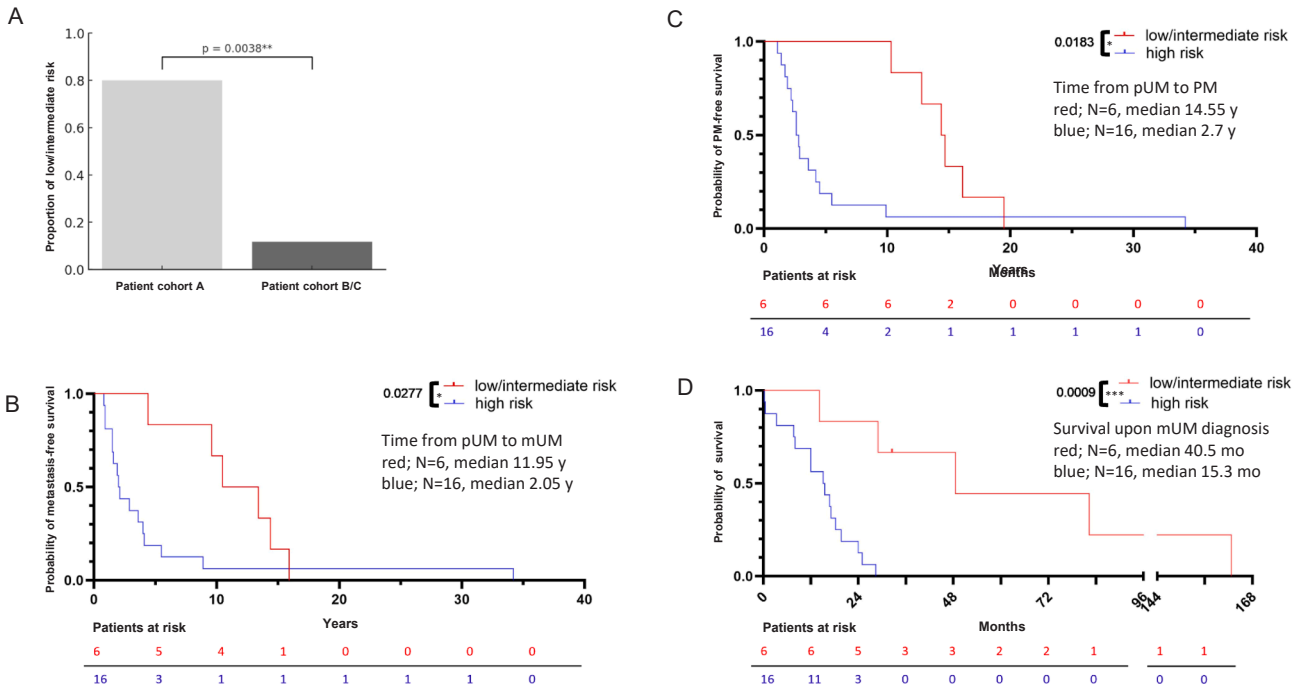

Fig. 5. Clinical course according to tumor genetic risk group. (A) Proportion of patients with low/intermediate genetic risk among cohort A (light grey) and cohort B/C (dark grey). Mann-Whitney U Test: p = 0.0038. Kaplan-Meier plots comparing patients with low/intermediate tumor genetic risk (red, N = 6) and high risk (blue, N = 16) representing (B) metastasis-free survival from primary UM diagnosis (median 11.95 vs. 2.05 years, p = 0.0277), (C) PM-free survival from primary UM diagnosis (median 14.55 vs. 2.7 years, p = 0.0183), (D) overall survival from diagnosis of metastatic disease (median 40.5 vs. 15.3 months, p = 0.0009). Log-rank (Mantel Cox) test.

months in the control group) [8,9]. Interestingly, only 19.5 % of patients in our cohort received treatment with tebentafusp resulting in a median PFS of three months (data not shown).

Moreover, within a small subgroup of patients with initial sole extrahepatic spread at the time of mUM diagnosis, we observed an exceptionally long median OS of 48.6 months, which was significantly longer compared to the OS in patients with initial liver metastases, irrespective of simultaneous or subsequent extrahepatic spread.

Interestingly, in a phase II trial of patients undergoing first-line dual ICB treatment, a longer OS was also observed in patients with extrahepatic metastases compared to patients with exclusive liver metastases and those with both liver and extrahepatic metastases (23.5 vs. 9.2 vs. 15.5 months), respectively, although this was not significant [34]. A similar trend was observed in a retrospective study of 178 mUM patients undergoing dual ICB treatment [35]. In accordance with this, we observed a tendency towards a longer PFS under ICB treatment in patients with sole extrahepatic dissemination compared to patients with liver affection at the time of diagnosis of metastatic disease, although this missed statistical significance. When interpreting these data, it is important to note that the number of ICB-treated patients in our study was limited (N = 17). We did not observe a correlation between PFS under ICB and TMB. However, TMB was only available in 10 patients. This point should be prospectively addressed in larger cohorts.

Metastatic patterns seem to reflect prognostically different subgroups of mUM patients [36]. This can partly be explained by the immunosuppressive microenvironment of the liver on the one hand and particular immunological tumor characteristics on the other [13]. In CM, liver metastases were shown to be the least responsive of metastatic sites to dual ICB treatment [37]. Compared to CM, UM liver metastases comprise an even higher ratio of exhausted $CD8^+$ T cells to cytotoxic T cells and to Th1 cells, despite a similar extent of immune cell infiltrates [38]. Moreover, PD-L1 expression as well as tumor mutational burden and thus neoantigen load is known to be comparably low in UM liver metastases [38]. Our immunohistochemical analysis of UM liver metastases confirmed the observation that infiltrating leukocytes are mainly comprised of $CD8^+$ T cells and macrophages and low percentages or even absence of B and NK cells [39]. Unfortunately, only 1 PM sample was available for analysis of the immune cell composition. However, there is growing evidence in UM, that immune cell infiltrates differ according to the metastatic site, e.g. with lower densities of total $CD8^+$ T cells and macrophages in extrahepatic metastases compared to liver metastases [39]. Yet, comprehensive analyses to potentially explain differences in response to immune checkpoint blockade in regard to metastatic sites including PM are lacking thus far. Unfortunately, owing to the retrospective character and low sample size of available tumor tissue, we are unable to make any statements regarding a possible correlation between the genetic risk group, metastatic site and $CD8^+$ frequency. Existing information in available tumor samples is displayed in Table S3.

In the context of mUM an inflammatory phenotype is associated with poor prognosis [14,15]. Interestingly, it has been shown that T-cell infiltrates are associated with BAP1-inactivated melanomas [40,41]. BAP1 loss and the absence of its deubiquitinating function were shown to be correlated with upregulation of the NFkB pathway, followed by upregulation of HLA class I expression and attraction of immune cells to the tumor microenvironment, thus causing an inflammatory phenotype [41]. There is further evidence that suggests a considerable link between tumor genetics and the tumor immune contexture in UM, such as the influx of macrophages in tumors with a gain of chromosome 8q [41]. In our cohort, time to metastasis as well as time to PM from primary UM and survival upon mUM diagnosis was longest in patients with initial extrahepatic spread, potentially indicating an underlying favourable tumor biology. We could substantiate these assumed differences in tumor biology reflected by distinct metastatic patterns by the observation that tumors with low and intermediate genetic risk were significantly overrepresented in patients with initial sole extrahepatic metastases (cohort A). The significant impact of tumor genetics on the clinical progression of uveal melanoma (UM) is highlighted by our findings, that patients with tumors of low and intermediate genetic risk show a significantly better prognosis than high-risk tumors, not only in

regard to metastasis-free survival, but also regarding OS upon mUM diagnosis.

While our analyses of the clinical courses of mUM regarding the occurrence of PM revealed different prognostic subgroups, the specific role of PM as an extrahepatic site, compared to other extrahepatic locations, remains unclear. Exclusively extrahepatic metastatic spread could be linked to a generally more favorable prognosis, regardless of the extrahepatic sites involved.

Further research is needed in larger patient cohorts to decipher the complex interplay of immunogenomics and the respective impact of coexisting factors on UM prognosis.

5. Conclusion

In contrast to other extra-abdominal cancers, PM in UM was not associated with adverse OS. The observation that the prognosis of mUM with extrahepatic disease was considerably better in the absence or rather late occurrence of liver metastases seems to be confirmed in mUM patients with PM. Underlying tumor genetics have the potential to delineate UM subgroups with distinct clinical features as shown here. Further research focusing on the interconnection between tumor genetics and tumor immune cell composition in different metastatic sites could result in patient stratification for biomarker-informed treatment in the future.

Funding

SMR was participant in the BIH Charité Clinician Scientist Program funded by the Charité – Universitätsmedizin Berlin, and the Berlin Institute of Health at Charité (BIH) and received funding from the Lydia-Rabinowitsch grant and the gender-equality fund of the Charité Universitätsmedizin Berlin. CP and JI are currently participating in the BIH Charité Clinician Scientist Program funded by the Charité – Universitätsmedizin Berlin, and the Berlin Institute of Health at Charité (BIH).

CRediT authorship contribution statement

Stanislav Rosnev: Writing – review & editing, Writing – original draft, Visualization, Formal analysis, Data curation, Conceptualization. **Caroline A. Peuker:** Writing – review & editing, Writing – original draft, Resources, Conceptualization. **Iris Piwonski:** Writing – review & editing, Formal analysis. **Jana Ihlow:** Writing – review & editing, Formal analysis. **Serge Leyvraz:** Writing – review & editing, Resources. **Jonas Klingberg:** Writing – review & editing. **David Horst:** Writing – review & editing. **Maria Joosten:** Resources. **Markus Möbs:** Resources. **Antonia M. Joussen:** Writing – review & editing. **Maximilian de Bucourt:** Writing – review & editing. **Ulrich Keilholz:** Writing – review & editing. **Ulrich Keller:** Writing – review & editing, Supervision, Resources. **Sebastian Ochsenreither:** Writing – review & editing, Supervision, Resources, Conceptualization. **Susanne M. Rittig:** Writing – review & editing, Writing – original draft, Visualization, Supervision, Resources, Formal analysis, Conceptualization.

Declaration of Competing Interest

The authors declare that they have no known competing financial interests or personal relationships that could have appeared to influence the work reported in this paper. author is an Editorial Board Member/Editor-in-Chief/Associate Editor/Guest Editor for this journal and was not involved in the editorial review or the decision to publish this article. CP and UKei received financial support for an investigator-initiated trial in mUM patients (EudraCT-Number: 2014–002439–32) from Sirtex and PharmaCept (now Magle PharmaCept). UKei is an Editorial Board Member for this journal and was not involved in the editorial review or the decision to publish this article. SO received financial compensation from Immunocore for participating in advisory boards. The other authors declare that they have no competing financial interests.

Appendix A. Supporting information

Supplementary data associated with this article can be found in the online version at doi:10.1016/j.ejca.2025.115280.

References

[1] Jager MJ, et al. Uveal melanoma. Nat Rev Dis Prim 2020;6:24.
[2] Jensen OA. Malignant melanomas of the human uvea: 25-year follow-up of cases in Denmark, 1943–1952. Acta Ophthalmol (Copenh) 1982;60:161–82.
[3] Kujala E, Makitie T, Kivela T. Very long-term prognosis of patients with malignant uveal melanoma. Invest Ophthalmol Vis Sci 2003;44:4651–9.
[4] Kolandjian NA, et al. Delayed systemic recurrence of uveal melanoma. Am J Clin Oncol 2013;36:443–9.
[5] Collaborative Ocular Melanoma Study G. Assessment of metastatic disease status at death in 435 patients with large choroidal melanoma in the Collaborative Ocular Melanoma Study (COMS): COMS report no. 15. Arch Ophthalmol 2001;119:670–6.
[6] Wei AZ, et al. Characterizing metastatic uveal melanoma patients who develop symptomatic brain metastases. Front Oncol 2022;12:961517.
[7] Rantala ES, Hernberg M, Kivela TT. Overall survival after treatment for metastatic uveal melanoma: a systematic review and meta-analysis. Melanoma Res 2019;29:561–8.
[8] Nathan P, et al. Overall survival benefit with tebentafusp in metastatic uveal melanoma. N Engl J Med 2021;385:1196–206.
[9] Hassel JC, et al. Three-year overall survival with tebentafusp in metastatic uveal melanoma. N Engl J Med 2023;389:2256–66.
[10] Harbour JW, et al. Frequent mutation of BAP1 in metastasizing uveal melanomas. Science 2010;330:1410–3.
[11] Jager MJ, Brouwer NJ, Esmaeli B. The cancer genome Atlas project: an integrated molecular view of uveal melanoma. Ophthalmology 2018;125:1139–42.
[12] Thorsson V, et al. The immune landscape of cancer. e814 Immunity 2018;48:812–30. e814.
[13] Yarchoan M, Hopkins A, Jaffee EM. Tumor mutational burden and response rate to PD-1 inhibition. N Engl J Med 2017;377:2500–1.
[14] Robertson AG, et al. Integrative analysis identifies four molecular and clinical subsets in uveal melanoma. e215 Cancer Cell 2017;32:204–20. e215.
[15] Maat W, et al. Monosomy of chromosome 3 and an inflammatory phenotype occur together in uveal melanoma. Invest Ophthalmol Vis Sci 2008;49:505–10.
[16] Davidorf FH, Lang JR. Lymphocytic infiltration in choroidal melanoma and its prognostic significance. Trans Ophthalmol Soc U K (1962) 1977;97:394–401.
[17] Niederkorn J, Streilein JW, Shadduck JA. Deviant immune responses to allogeneic tumors injected intracamerally and subcutaneously in mice. Invest Ophthalmol Vis Sci 1981;20:355–63.
[18] Niederkorn JY. Immune escape mechanisms of intraocular tumors. Prog Retin Eye Res 2009;28:329–47.
[19] Yamada K, et al. Immune checkpoint inhibitors for metastatic uveal melanoma: a meta-analysis. Sci Rep 2024;14:7887.
[20] Khan S, Carvajal RD. Dual immunological checkpoint blockade for uveal melanoma. J Clin Oncol 2021;39:554–6.
[21] Rowcroft A, Loveday BPT, Thomson BNJ, Banting S, Knowles B. Systematic review of liver directed therapy for uveal melanoma hepatic metastases. HPB (Oxf) 2020;22:497–505.
[22] Carvajal RD, et al. Clinical and molecular response to tebentafusp in previously treated patients with metastatic uveal melanoma: a phase 2 trial. Nat Med 2022;28:2364–73.
[23] Howlett S, Carter TJ, Shaw HM, Nathan PD. Tebentafusp: a first-in-class treatment for metastatic uveal melanoma. Ther Adv Med Oncol 2023;15:17588359231160140.
[24] Bootsma S, Bijlsma MF, Vermeulen L. The molecular biology of peritoneal metastatic disease. EMBO Mol Med 2023;15:e15914.
[25] Hennessy BT, Coleman RL, Markman M. Ovarian cancer. Lancet 2009;374:1371–82.
[26] Rijken A, et al. Peritoneal metastases from extraperitoneal primary tumors: incidence, treatment, and survival from a nationwide database. Indian J Surg Oncol 2023;14:60–6.
[27] Flanagan M, et al. Peritoneal metastases from extra-abdominal cancer - a population-based study. Eur J Surg Oncol 2018;44:1811–7.
[28] Willing EM, et al. Development of the NOGGO GIS v1 assay, a comprehensive hybrid-capture-based NGS assay for therapeutic stratification of homologous repair deficiency driven tumors and clinical validation. Cancers (Basel) 2023;15.
[29] Chalmers ZR, et al. Analysis of 100,000 human cancer genomes reveals the landscape of tumor mutational burden. Genome Med 2017;9:34.
[30] Beniey M. Peritoneal metastases from breast cancer: a scoping review. *Cureus* 2019;11:e5367.
[31] Siragusa L, et al. Therapeutic strategies and oncological outcome of peritoneal metastases from lung cancer: a systematic review and pooled analysis. Curr Oncol 2023;30:2928–41.
[32] Khoja L, et al. Meta-analysis in metastatic uveal melanoma to determine progression free and overall survival benchmarks: an international rare cancers initiative (IRCI) ocular melanoma study. Ann Oncol 2019;30:1370–80.

[33] Kivela TT, et al. Validation of a prognostic staging for metastatic uveal melanoma: a collaborative study of the European Ophthalmic Oncology Group. Am J Ophthalmol 2016;168:217–26.
[34] Piulats JM, et al. Nivolumab Plus Ipilimumab for Treatment-Naive Metastatic Uveal Melanoma: An Open-Label, Multicenter, Phase II Trial by the Spanish Multidisciplinary Melanoma Group (GEM-1402). J Clin Oncol 2021;39:586–98.
[35] Koch EAT, et al. Immune checkpoint blockade for metastatic uveal melanoma: patterns of response and survival according to the presence of hepatic and extrahepatic metastasis. Cancers (Basel) 2021;13.
[36] Koch EAT, et al. Clinical determinants of long-term survival in metastatic uveal melanoma. Cancer Immunol Immunother 2022;71:1467–77.
[37] Pires da Silva I, et al. Site-specific response patterns, pseudoprogression, and acquired resistance in patients with melanoma treated with ipilimumab combined with anti-PD-1 therapy. Cancer 2020;126:86–97.
[38] Hoefsmit EP, et al. Comprehensive analysis of cutaneous and uveal melanoma liver metastases. J Immunother Cancer 2020;8.
[39] Tosi A, et al. The immune cell landscape of metastatic uveal melanoma correlates with overall survival. J Exp Clin Cancer Res 2021;40:154.
[40] Bronkhorst IH, et al. Different subsets of tumor-infiltrating lymphocytes correlate with macrophage influx and monosomy 3 in uveal melanoma. Invest Ophthalmol Vis Sci 2012;53:5370–8.
[41] Gezgin G, et al. Genetic evolution of uveal melanoma guides the development of an inflammatory microenvironment. Cancer Immunol Immunother 2017;66:903–12.